

The Niger River Basin Moisture Sources. A Lagrangian Analysis

Rogert Sorí ^{1,*}, Raquel Nieto ^{1,2}, Anita Drumond ¹ and Luis Gimeno ²

Published: 15 July 2016

¹ Environmental Physics Laboratory (EPhysLab), Facultad de Ciencias, Universidade de Vigo, Ourense, Spain

² Department of Atmospheric Sciences, Institute of Astronomy, Geophysics and Atmospheric Sciences, University of São Paulo, São Paulo, Brazil

* Correspondence: rogert.sori@uvigo.es

Abstract: The Niger River basin (NRB) is located on the important climatic region of the African Sahel. In this work we use the Lagrangian tridimensional model FLEXPART v9.0, to identify and characterize the moisture sources for the NRB. The method allowed integrating the evaporation minus precipitation budget through 10 days backward trajectories and thus, identifying the origin of air masses residing over the NRB. The analysis was performed for 35 years from 1980 to 2014. There were identified the main seasonal climatological moisture sources of the NRB and quantify their contribution to the total moisture influx. At first day backward in time the NRB appears as the main moisture source, contributing less and less humidity to the particles during last days, suggesting the importance of local moisture supply to recycling process. Through the 10 days backward, the pattern of (E – P) shows the spatial expansion of sources and sinks regions. Across the year, the moisture supply to the NRB mainly comes from itself and the tropical-east south Atlantic Ocean, but are also important the rest of the sources located on the tropical-east north Atlantic Ocean near Africa, the Sahel surrounded regions, the Mediterranean Sea, the east Africa, the north-east Africa and less important small regions on central-equatorial Africa and the tropical-west Indian Ocean.

Keywords: moisture sources; Lagrangian analysis; Niger River Basin

1. Introduction

On the western Africa, the Niger River basin (NRB) is shared by nine countries and divided into four major sections, namely Upper Niger, Inland Delta, Middle Niger, and Lower Niger covering the 7.5% of the African continent [1]. Between the meridians of 11°30' west and 15° east, from Guinea to Chad; and between the parallels of 22° north and 5° north, from the Hoggar Mountains to the Gulf of Guinea [2] the NRB is located in the African Sahel (Figure 1). The Sahel is a transition zone between the Saharan desert and the wet climate of tropical Africa [3] giving to the basin a contrasting climatic conditions mostly varying with latitude. According with the climatic classification of L'Hôte and Mahé [4] for West Africa (WA) based on the annual rainfall, the NRB experiments five climatic zones with a transition between Deserts (arid) from the north, until Transitional equatorial in the south. From June to November (wet season), the rises of the Saint Helena high-pressure area toward the north, signals the beginning of the monsoon season with humid and unstable maritime equatorial air and relatively cool temperatures [2]. The monsoons are longer and wetter in the southern part of the basin [1]. From December to May is the dry season; under the influence of the Saharan high-pressure zone, the northeastward harmattan wind brings hot dry air and high temperatures which last longer in the north [2].

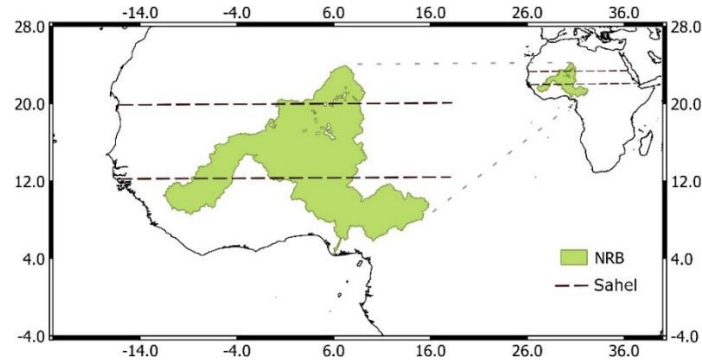


Figure 1. Geographical location of the Niger River Basin in Western Africa.

The mean annual precipitation ranges from less than 50 mm/year in the northern portion of the basin in Algeria, increasing southward until more than 2000 mm/year close to the river mouth in the Guinean/coaster zone [2]. The observed annual average precipitation changes in the period 1951–2010 over Africa [5], show negative trends in areas of the NRB. The major circulation features associated with the variability of the Sahel rainfall on interannual and decadal time scales, are the upper-level Tropical Easterly Jet, the mid-level African Easterly Jet and the Saharan heat low; while a relationship to the intensity of the Intertropical Convergence Zone (ITCZ) (as defined by rainfall intensity) result apparent [6]. Studies addressing the climate variability in WA show the seasonal rainfall migration during the summer season [7] and a reduction in accumulate over the last century [5,8–10]. This fact affects the stream discharges and both are considered a partial feedback of the land-cover degradation in the watershed [11]. Nevertheless, a review of recent studies of the rainfall regime on the West African Sahel performed by Nicholson [6] showed some degree of recovery since the extreme dry episode of the 1970s and 1980s, but certain changes on the rainfall regime like less spatial coherence and less temporal persistence.

There is a large consensus that in WA one of the major climate change impacts will be on rainfall, making it more variable and less reliable [12]. West African precipitation projections in the CMIP3 and CMIP5 archives show inter-model variation in both the amplitude and direction of change, which is partially attributed to the inability of Global Climate Models (GCMs) to resolve the convective rainfall [5]. Although results of Oguntunde and Abiodun [13] suggest that under enhanced Greenhouse Gases (GHGs, specifically in an A1B scenario), the local evaporation will contribute less to atmospheric moisture and precipitation over the NRB. According to Gong and Elthair [14] the rainfall over any land region is contributed by two sources: the water vapor that is advected into the region from the surrounding areas, and the water vapor that is supplied by evaporation from the same region. And despite of some authors have studied the moisture sources for the Sahel region [15–17], taking into account the concern about climate predictions and the environmental and socioeconomic importance of the NRB, the goal of this work is to identify and characterize the moisture sources of the Niger River Basin. Studying the atmospheric branch of the hydrological cycle on the NRB will support studies of rainfall variability, runoff and rivers discharges.

2. Experiments

2.1. Method

Was utilized the Lagrangian particle dispersion model FLEXPART v9.0 developed by Stohl and James [17,18]. The model considers the atmosphere divided homogeneously into three dimensional finite elements (hereafter “particles”), each representing a fraction of the total atmospheric mass [17]. It allows obtain atmospheric moisture changes along backward and forward trajectories of air particles, permitting to establish a meaningful source-receptor relationships. In our case, was

performed the backward analysis from particles residing over the NRB, limiting the transport time to 10 days, according to the average residence time of the water vapor in the atmosphere [19]. This way, the rate of moisture increases (through evaporation from the environment, e) or decreases (through precipitation, p) along the trajectory of the particles is calculated by changes of specific humidity (q) in the time (t) by the Equation (1), assuming constant the mass (m) of the particles.

$$(e - p) = m(dq/dt) \quad (1)$$

After integrate over a target area is possible to obtain the moisture changes of all particles in the atmosphere column, obtaining the surface freshwater flux diagnose, hereafter represented by $(E - P)$. Through the implemented backward analysis, regions where the particles gain humidity (evaporation exceeds precipitation) along their trajectories towards the target area, are considered moisture sources, while regions where particles lose humidity are considered moisture sinks. FLEXPART has been successfully applied for similar goals in several regions of the world like the Sahel [15], the Orinoco River Basin [20], in China [21], in the Amazon River Basin [22], and continental regions [23].

The budget of $(E - P)$ was calculated for two periods, the documented dry season from December to May (DJFMAM) and the wet season between June and November (JJASON). For both seasons was implemented the backward analysis from 1 to 10 days and integrated over the 10 days, $(E - P)_{i10}$.

A threshold to delimitate the boundaries of the sources was utilized, it was calculated as the percentile 90 (p_{90}) of the $(E - P) > 0$ values. This technique, previously applied by Drumond et al. [21] ensures to select the regions where maximum evaporative values occur. In order to obtain the role of the NRB supplying humidity itself, was considered the whole basin as a source region.

2.2. Data

FLEXPART utilizes the ERA Interim reanalysis datasets [24] available at 6 h intervals (00, 06, 12, and 18 UTC) at a resolution of $1^\circ \times 1^\circ$ in 60 vertical levels, from 0.1 to 1000 hPa. The analysis was performed for 35 years from 1980 to 2014, supporting good climatological results. Datasets of precipitation in the basin (P_b) and the potential evapotranspiration (E_b), from the Climatic Research Unit (CRU 3.23TS) [25] were utilized to calculate the annual cycle of their balance in the NRB.

3. Results

3.1. Backward Analysis of $(E - P)$

The seasonal budget of the $(E - P)$ backward integrated from the Niger River basin from 1 to 10 days during the wet and dry season appears in Figure 2. In it, is possible to identify the spatial changes in moisture contribution to air masses each day before arrive to the NRB. The $(E - P) > 0$ areas are moisture sources regions while $(E - P) < 0$ are moisture sinks.

One day backward in time for both seasons, mainly the NRB itself acts as moisture source, but in the wet months the east part of the basin and Sahel regions mostly to the south of the NRB acts as moisture sinks, suggesting the occurrence of convective precipitation that typically occurs in air masses in transit to the Sahel [14]. At days 2 and 3 backward the resulting pattern of $(E - P)$ is characterized by positive values remaining over the NRB, extending across the Sahel, North Africa and parts of the Mediterranean Sea during both seasons, being more intense during wet months. In these days, areas where $(E - P) < 0$ are distributed along the equatorial Africa and the Atlantic Ocean being more intense between December and May, when the ITCZ moves southward during the austral summer [6]. At days 4 and 5 the spatial pattern of $(E - P)$ becomes greater. At these days in both seasons the NRB remains as moisture source and the east-equatorial South Atlantic Ocean covering the Gulf of Guinea becomes a common moisture source for both seasons, as well as the Mediterranean Sea. According with Schicker et al. [26] the Western North Africa receives less

Mediterranean rainwater than north-east and central Africa. Also for these days the tropical-east North Atlantic Ocean (NAtl) becomes into a wide moisture source region during DJFMAM.

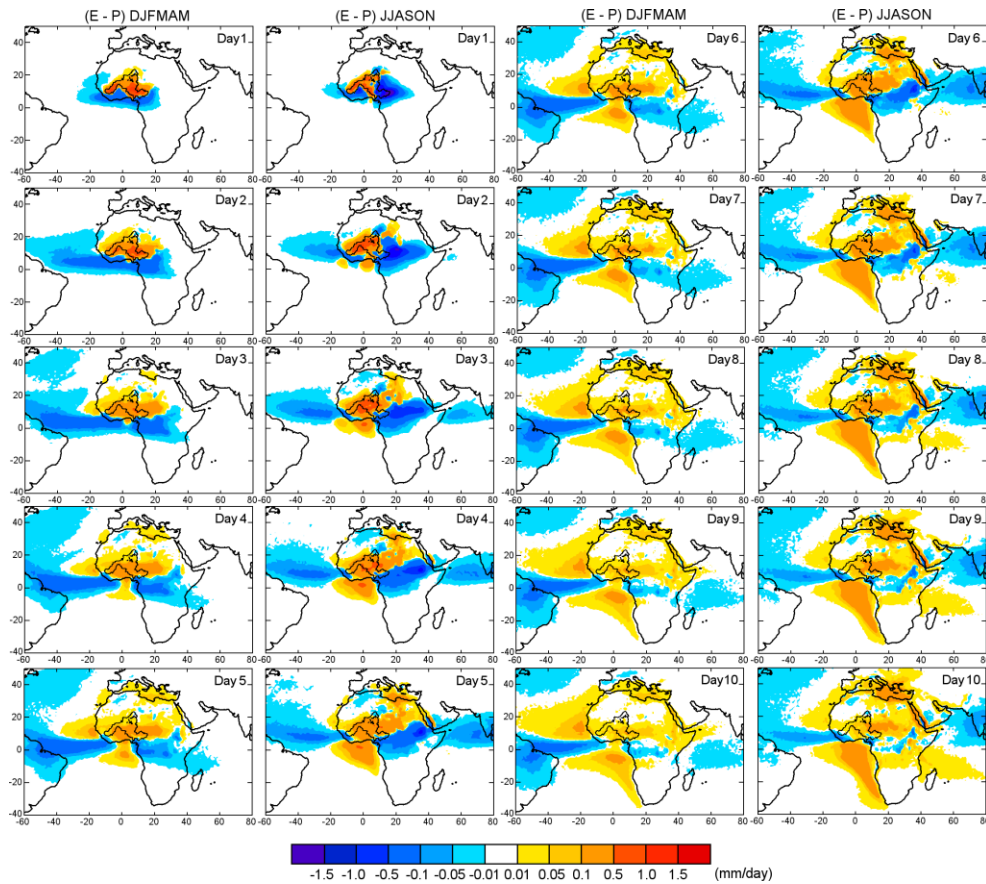


Figure 2. Seasonal pattern of $(E - P)$ backward integrated from the Niger River Basin for days 1 to 10, during DJFMAM (dry months) and JJASON (wet months).

From day 6 and following backward days is possible to observe that regions where particles lose moisture to the atmosphere before reach the NRB are more intense around the equatorial Atlantic Ocean and central Africa. The greatest differences observed on the $(E - P) > 0$ areas between DJFMAM and JJASON are well distinguished in the NAtl region, where in the wet season the spatial pattern is confined to the African coast but in dry months propagates to the west until reach the Caribbean by day 10. In the last three days (8 to 10) is more clearly appreciated in the dry season that part of the Arabian Sea supply moisture to particles traveling to the NRB, but the opposite occurs in the wet season of the NRB when the Arabian Sea turns as an important moisture source for precipitation to the Indian monsoon [27]. Besides for JJASON, in the west-tropical Indian Ocean between 0° and 10° S, a small region with $(E - P) > 0$ values, expands to the east from day 6 backward until day 10, when reached the 20° LS. Despite of sources regions varies or persists along 10 days, part of the uptake of moisture of the NRB from them, can fall as precipitation along the trajectories of the air masses as they move towards the target area [28]. In general, is appreciated that $(E - P) > 0$ values in the wet season are more intense. Areas with positive values of $(E - P)$ are more intense in wet months than in dry months when rainfall increases over the basin. A common characteristic of the $(E - P)$ pattern for both season since first backward days is the persistence of moisture contribution from the NRB itself, which suggest their role on local recycling process, documented to be the dominant moisture source over the Sahel [15].

3.2. Seasonal ($E - P$)

As a way to summarize daily results, was integrated in 10 days the budget of ($E - P$) for each season, represented in Figure 3 like ($E - P$)_{i10}. The pattern of ($E - P$)_{i10} in Figure 3a,b, is very similar with the obtained for the 10th day in Figure 2. In both, the p90 of the ($E - P$) > 0 values is represented by a magenta line that identifies predominantly evaporative regions (Figure 3), those finally utilized as moisture sources for the target area and clearly showed in Figure 4. From December to May (Figure 4a) the p90 = 0.13 mm/day defines the following boundaries of the sources regions: the “tropical-east north Atlantic Ocean” (NAtl), the “tropical-east south Atlantic Ocean” (SAtl), to the west of the basin the “western Sahel” (WSah), the NRB, in the south of the basin the “southern Sahel” (SSah), to the east of the basin the “eastern Sahel” (ESah) and the “eastern Africa” (EA), and finally the “Mediterranean Sea” (MEDT). Indeed, during the wet season the sources now defined by the p90 = 0.10 mm/day have changed mainly their spatial extension (Figure 4b). It is well appreciated in the boundaries of the MEDT source, which is expanded to the north in Europe, the SAtl to the south and the NAtl have reduced and confined near the African coasts. Besides, appears new small sources in “Central Africa” (CEA) and the “Indian Ocean” (Ind). The name assigned to the sources regions is in accordance to the place it is located.

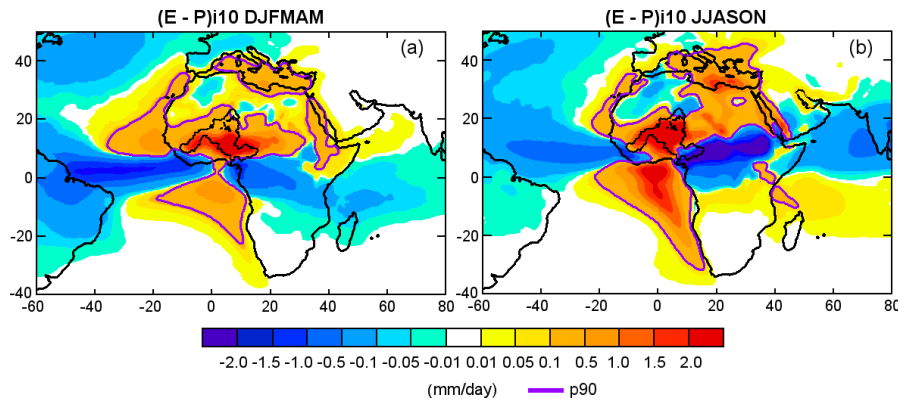


Figure 3. Average pattern of ($E - P$) backward integrated from the Niger River Basin for days 10 during the dry (a) and wet season (b). The magenta line represents the percentile 90 of ($E - P$)_{i10} > 0 values, p90 = 0.13 mm/day (a) and p90 = 0.10 mm/day (b).

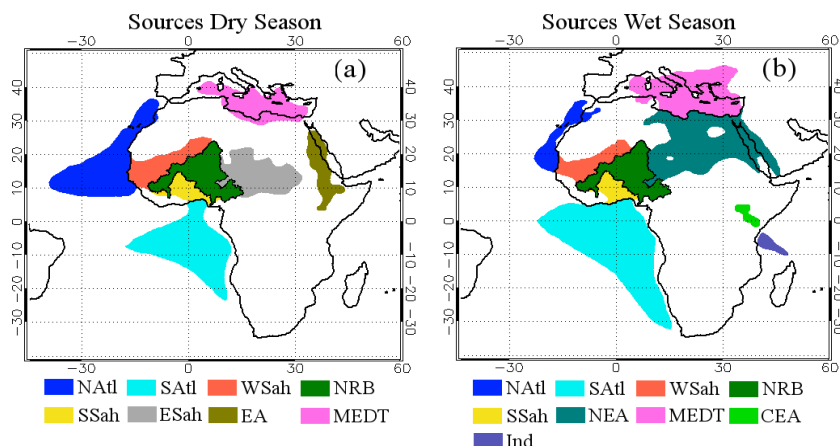


Figure 4. Moisture sources for the NRB during the dry season (a) and wet season (b).

Because of precipitation in route, earlier evaporative sources of moisture will contribute less and less to the precipitation at the arrival site; hence the precipitation at the target area is a weighted sum of the previous uptakes [29]. This behavior is also appreciated in Figure 5, where is represented the daily budget of ($E - P$) on air masses for 10 days before arrive to the NRB from the sources, which

not exactly means the precipitation rate. First common sources identified since one and two backward days (Figure 2) the NRB, WSah, SSah and ESah, are the main responsible supplying humidity to the air on first's days for both seasons, while it decreases during last days. On the opposite, sources like the SATl and the MEDT acts as moisture sinks at first's days but after the 3rd backward day, they start to provide moisture to the particles (specially in JJASON). According with the intensity of the resulting budget of $(E - P)$ in Figure 2, and the average budget for both seasons in Figure 5, the moisture contribution of the NRB to itself during first's days back in time is greater than the rest in DJFMAM (Figure 5a), showing the importance of local recycling. On the contrary in the wet season it becomes a moisture sink the first day (Figure 5b). After the 6th day in dry season and 4th in wet season, the SATl becomes the most important region on the moisture contribution to the NRB. Some sources like the Ind and CEA have not relevant contributions.

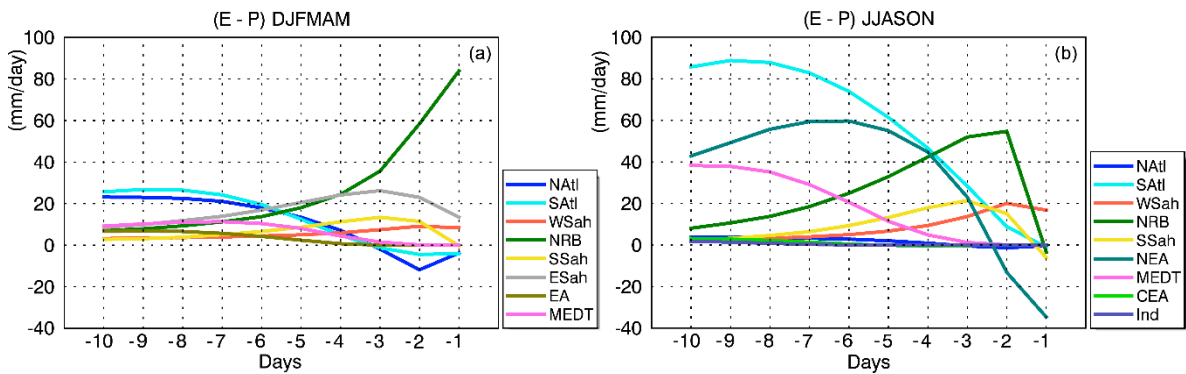


Figure 5. Climatological seasonal (dry (a) and wet (b)) average of 10 days integrated $(E - P)$ obtained through the backward analysis from the NRB over the moisture sources, in the period 1980–2014.

3.3. Monthly $(E - P)_{i10}$

The source-receptor relationship was also addressed through the monthly average of $(E - P)_{i10}$ backward obtained from the NRB over the sources (Figure 6), already defined for each climatic season. Some of these sources change spatially between dry and wet season, and other appears just during one; hence colors in Figure 6 not only represent the season if not also different spatial extension between the sources (Figure 4). As commented the only source defined without spatial changes along the year was the own NRB, like a way to evaluate itself.

Analyzing the sources starting from the west to the east, the NATl and SATl play a different role across the year. The NATl provides the maximum moisture contribution along dry months (Figure 6a) when it's more extended to the west in the ocean (Figure 4a), and reach a peak of 18 mm/day in January to later decrease the contribution in next months. From June to November this source experiment a spatial reduction (Figure 4b), and with this, a decrease on the moisture contribution (<5 mm/day) becoming a moisture sink in September.

The SATl source as was expected, has the opposite cycle of the NATl budget of $(E - P)_{i10}$; with minor values in dry months that increase month by month until May (~30 mm/day) (Figure 6b). In the wet season when the boundaries ho delimited this source extends to the south under the 30° S (Figure 4b) the moisture supply turns elevated, being maximum in August (~100 mm/day). In November this source acts as moisture sink. This behavior follows the monsoon period in the African Sahel, when southerly winds transport moisture from the Gulf of Guinea [30]. These results are agreeing whit similar analysis for the whole Sahel region developed by Nieto et al. [15].

The WSah region despite to remain without huge spatial changes between dry and wet months (Figure 4); the monthly average of $(E - P)_{i10}$ over this source reflects that in general, it contributes with less moisture to air parcels on their travel to the basin during dry months (Figure 6c). From December onward there is an increasing moisture contribution until May (~11.5 mm/day),

followed by a decrease in the first month of the wet season, although in July and August achieve the maximum annual contribution (>13 mm/day), that later declines.

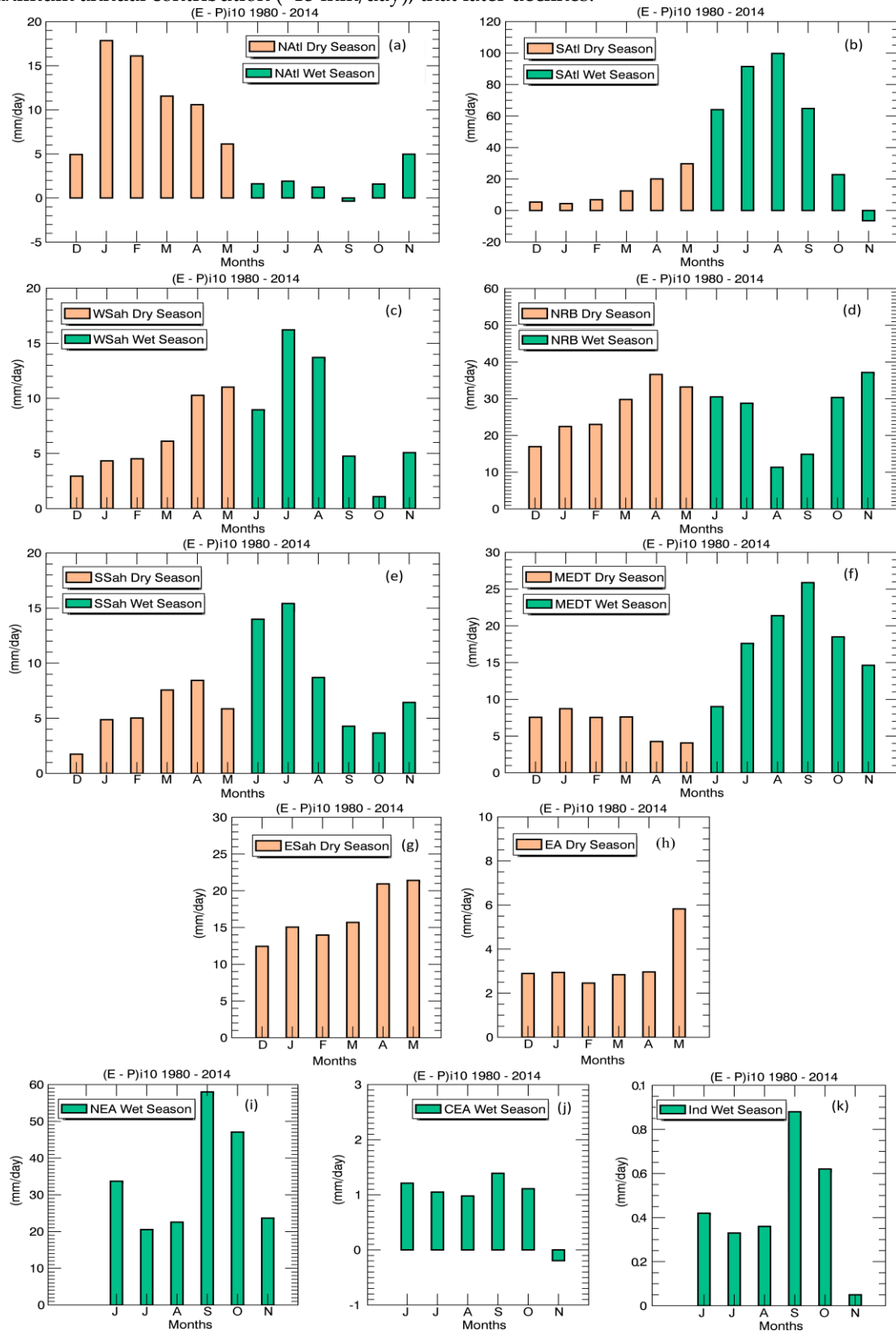


Figure 6. Climatological monthly average of 10 days (E - P) integrated backward from the Niger River Basin over the identified sources in the dry and wet seasons. Period 1980–2014.

In the NRB as average, itself is able to provide moisture to the atmospheric column during all months of the year, with an annual cycle characterized by two maximum of around 40 mm/day in April and November and a minimum in August (~11 mm/day) (Figure 6d), when precipitation exceeds evaporation in the NRB (Figure 7).

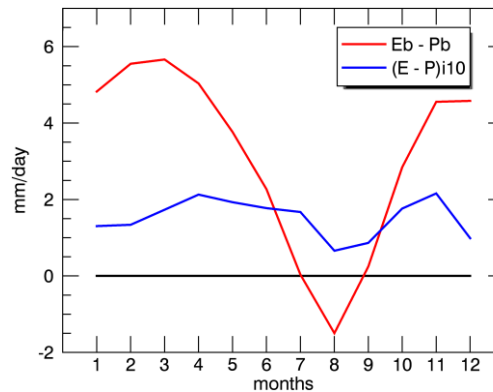


Figure 7. Annual cycle of Evaporation minus Precipitation spatially averaged in the NRB from data of CRU 3.23TS (red line) and estimated by FLEXPART (blue line).

In the south of the NRB on the SSah, from December onward positive values of $(E - P)i10$ increase until April (~8 mm/day) and decrease in May the last month of the dry season (Figure 6e). The wet season starts, and on June and July the $(E - P)i10 > 14$ mm/day but in later months the budget diminishes.

The MEDT source has a clear differentiate role characterized by an important contribution of moisture to the NRB during JJASON (wet season). As average a maximum contribution occurs in September (~27 mm/day) and less during dry months with a minimum in May (~4 mm/day) (Figure 6f). The last sources remain during the both seasons but they change in extension according to the visual analysis in Figure 4.

In the ESah, a region only identified for dry months, the budget of $(E - P)i10$ increases from December (~12.5 mm/day) to May (~22 mm/day) (Figure 6g) while in the EA region the contributions are less with a maximum in May when reach almost 6 mm/day (Figure 6h). In the wet season the last two sources joint into one and moved to the north-east Africa; the source now called NEA is characterized by highest contribution of moisture in September and October (>45 mm/day) (Figure 6i). Other small sources regions that only appear in the wet season, the CEA (Figure 6j) and the Ind (Figure 6k) seems to follow the same cycle of $(E - P)i10$ budget, with a common maximum contribution in September but finally without an important role on the moisture uptake of the NRB.

3.4. Annual Cycle of $E - P$ in the NRB

The monthly spatial average of the atmospheric budget of $(E - P)i10$ over the NRB, obtained with FLEXPART is represented in Figure 7; together with the local budget of $(Eb - Pb)$ obtained with data of precipitation and potential evapotranspiration from CRU. The balance of $(Eb - Pb)$ follows an annual cycle with two maximum peaks in March and December while reach the minimum and negative value in August, when the maximum rainfall occur in the NRB (graph not shown) and the Sahel [6]. August is the only month when the average rainfall exceeds the mean evaporation rate of the month. FLEXPART is also able to distinguish an annual cycle with two peaks of maximum values, but in April and November; besides occurs a minimum in the annual balance in August, but the

$(E - P)i10$ values remain positive in all months. This is agree with previous discussed results, that even during the wet season the own NRB as a whole acts as an effective moisture source for itself.

4. Conclusions

The main moisture sources for the Niger River Basin were identified and investigated through a Lagrangian approach. The analysis was carried out for 35 years (1980–2014) taking into account the documented rainfall annual cycle in basin; from December to May (dry season) and from June to November (wet season). After track the air residing over the NRB 10 days back in time in the dry season, we obtained that it acts as the main responsible region supplying moisture itself during the first 4 days backward, as well as the surrounded regions of the Sahel. In the wet season, on the east part of the NRB occur moisture sink at first backward day, but later this changes and affords moisture like the Sahel surrounded sources areas does. From the first to the tenth day, the extension of the moisture sources and sinks increase. The resulting budget of the (E – P) backward integrated 10 days from the NRB permitted to identify the main moisture sources of the NRB across the year. The NATl, SATl, WSah, SSah, ESah, EA, NEA and the MEDT regions were identified as moisture sources during both seasons, but their spatial extension differs and as consequence the monthly average in the budget of (E – P)₁₀ varies. These averages confirm that for the whole year the NRB and the SATl regions are the most important zones contributing to the moisture uptake of the NRB. Other regions like the MEDT are more important supplying humidity from June to November while the NATl during dry months. The small regions in central Africa and the Indian Ocean that acts as moisture sources only for wet months are not relevant on the total moisture influx to the NRB. Further analysis are required to deeply understand the influence of atmospheric circulation mechanism on moisture transport from these sources to the NRB, as well as their role during extremes events like droughts episodes, floods and extreme river discharge.

Acknowledgments: R.S. thanks the grant received by the Xunta of Galicia, Spain, to support the doctoral research work and R.N. acknowledges the support of the CNPq grant 314734/2014-7 by the Brazilian government.

Author Contributions: R.N., A.D. and L.G. designed, proposed and conducted the research; R.S. performed the experiments and analyzed the data; R.S., R.N., L.G. and A.D. wrote the paper.

Conflicts of Interest: The authors declare no conflict of interest. The funding sponsors had no role in the design of the study; in the collection, analyses, or interpretation of data; in the writing of the manuscript, and in the decision to publish the results.

Abbreviations

The following abbreviations are used in this manuscript:

NRB	Niger River Basin
WA	West Africa
NATl	Tropical-east North Atlantic Ocean
SATl	Tropical-east South Atlantic Ocean
WSah	Western Sahel
SSah	Southern Sahel
ESah	Eastern Sahel
EA	Eastern Africa
MEDT	Mediterranean Sea
NEA	North-east Africa
CEA	Central-east Africa
Indian Ocean	Ind

References

1. Namara, R.E.; Barry, B.; Owusu, E.S.; Ogilvie, A. *An Overview of the Development Challenges and Constraints of the Niger Basin and Possible Intervention Strategies*; IWMI Working Paper 144; International Water Management Institute: Colombo, Sri Lanka, 2011; p. 34, doi:10.5337/2011.206.
2. Andersen, I.; Dione, O.; Jarosewich-Holder, M.; Olivry, J.-C. *The Niger River Basin: A Vision for Sustainable Management*; World Bank: Washington, DC, USA, 2005; doi:10.1596/978-0-8213-6203-7.

3. Buontempo, C. *Sahelian Climate: Past, Current, Projections*; Sahel and club west Africa Secretariat. 2010.
4. L'Hôte, Y.; Mahé, G. *Afrique de l'ouest et Centrale. Carte des Précipitations Moyennes Annuelles (Période 1951–1989)*; Office de la Recherche Scientifique et Technique d'Outre-Mer (ORSTOM): Paris, France, 1996.
5. Niang, I.; Ruppel, O.C.; Abdrabo, M.A.; Essel, A.; Lennard, C.; Padgham, J.; Urquhart, P. Africa. In *Climate Change 2014: Impacts, Adaptation, and Vulnerability. Part B: Regional Aspects*; Contribution of Working Group II to the Fifth Assessment Report of the Intergovernmental Panel on Climate Change; Cambridge University Press: Cambridge, UK; New York, NY, USA, 2014; pp. 1199–1265.
6. Nicholson, S.E. The West African Sahel: A Review of Recent Studies on the Rainfall Regime and Its Interannual Variability. *ISRN Meteorol.* **2013**, *2013*, 32, doi:10.1155/2013/453521.
7. Biasutti, M.; Yuter, S.E. Observed frequency and intensity of tropical precipitation from instantaneous estimates. *J. Geophys. Res. Atmos.* **2013**, *118*, 9534–9551, doi:10.1002/jgrd.50694.
8. Nicholson, S.E.; Some, B.; Kone, B. An analysis of recent rainfall conditions in West Africa, including the rainy seasons of the 1997 El Nino and the 1998 La Nina years. *J. Clim.* **2000**, *13*, 2628–2640.
9. Lebel, T.; Ali, A. Recent trends in the Central and Western Sahel rainfall regime (1990–2007). *J. Hydrol.* **2009**, *375*, 52–64.
10. Huang, J.; Zhang, C.; Prospero, J.M. Large-scale effect of aerosols on precipitation in the West African Monsoon region. *Q. J. R. Meteorol. Soc.* **2009**, *135*, 581–594.
11. Djebou, D.C.S. Integrated approach to assessing streamflow and precipitation alterations under environmental change: Application in the Niger River Basin. *J. Hydrol. Reg. Stud.* **2015**, *4*, 571–582, doi:10.1016/j.ejrh.2015.09.004.
12. Sarr, B. Present and future climate change in the semi-arid region of West Africa: A crucial input for practical adaptation in agriculture. *Atmos. Sci. Lett.* **2012**, *13*, 108–112, doi:10.1002/asl.368.
13. Oguntunde, P.G.; Abiodun, B.J. The impact of climate change on the Niger River Basin hydroclimatology, West Africa. *Clim. Dyn.* **2013**, *40*, 81–94, doi:10.1007/s00382-012-1498-6.
14. Gong, C.; Eltahir, E.A.B. Sources of Moisture for Rainfall in West Africa. *Water Resour. Res.* **1996**, *32*, 3115–3121.
15. Nieto, R.; Gimeno, L.; Trigo, R.M. A Lagrangian identification of major sources of Sahel moisture. *Geophys. Res. Lett.* **2006**, *33*, L18707, doi:10.1029/2006GL027232.
16. Salih, A.A.M.; Zhang, Q.; Tjernström, M. Lagrangian tracing of Sahelian Sudan moisture sources. *J. Geophys. Res. Atmos.* **2015**, *120*, 6793–6808, doi:10.1002/2015JD023238.
17. Stohl, A.; James, P. A Lagrangian analysis of the atmospheric branch of the global water cycle. Part 1: Method description, validation, and demonstration for the August 2002 flooding in central Europe. *J. Hydrometeorol.* **2004**, *5*, 656–678.
18. Stohl, A.; James, P. A Lagrangian analysis of the atmospheric branch of the global water cycle: 2. Earth's river catchments, ocean basins, and moisture transports between them, *J. Hydrometeorol.* **2005**, *6*, 961–984.
19. Numaguti, A. Origin and recycling processes of precipitating water over the Eurasian continent: Experiments using an atmospheric general circulation model. *J. Geophys. Res.* **1999**, *104*, 1957–1972.
20. Nieto, R.; Gallego, D.; Trigo, R.M.; Ribera, P.; Gimeno, L. Dynamic identification of moisture sources in the Orinoco basin in equatorial South America. *Hydrol. Sci. J.* **2008**, *53*, 602–617.
21. Drumond, A.; Nieto, R.; Gimeno, L. Sources of moisture for China and their variations during drier and wetter conditions in 2000–2004: A Lagrangian approach. *Clim. Res.* **2011**, *50*, 215–225, doi:10.3354/cr01043.
22. Drumond, A.; Marengo, J.; Ambrizzi, T.; Nieto, R.; Moreira, L.; Gimeno, L. The role of the Amazon Basin moisture in the atmospheric branch of the hydrological cycle: A Lagrangian analysis. *Hydrol. Earth Syst. Sci.* **2014**, *18*, 2577–2598, doi:10.5194/hess-18-2577-2014.
23. Gimeno, L.; Stohl, A.; Trigo, R.M.; Dominguez, F.; Yoshimura, K.; Yu, L.; Drumond, A.; Durán-Quesada, A.M.; Nieto, R. Oceanic and terrestrial sources of continental precipitation. *Rev. Geophys.* **2012**, *50*, RG4003, doi:10.1029/2012RG000389.
24. Dee, D.P.; Uppala, S.M.; Simmons, A.J.; Berrisford, P.; Poli, P.; Kobayashi, S.; Andrae, U.; Balmaseda, M.A.; Balsamo, G.; Bauer, P.; et al. The ERA-Interim reanalysis: Configuration and performance of the data assimilation system. *Q. J. R. Meteorol. Soc.* **2011**, *137*, 553–597, doi:10.1002/qj.828.
25. Harris, I.; Jones, P.D.; Osborn, T.J.; Lister, D.H. Updated high-resolution grids of monthly climatic observations—The CRU TS3.10 Dataset. *Int. J. Climatol.* **2014**, *34*, 623–642, doi:10.1002/joc.3711.
26. Schicker, I.; Radanovics, S.; Seibert, P. Origin and transport of Mediterranean moisture and air. *Atmos. Chem. Phys.* **2010**, *10*, 5089–5105, doi:10.5194/acp-10-5089-2010.

27. Levine, R.C.; Turner, A.G. Dependence of Indian monsoon rainfall on moisture fluxes across the Arabian Sea and the impact of coupled model sea surface temperature biases. *Clim. Dyn.* **2012**, *38*, 2167–2190.
28. Drumond, A.; Nieto, R.; Hernandez, E.; Gimeno, L. A Lagrangian analysis of the variation in moisture sources related to drier and wetter conditions in regions around the Mediterranean Basin. *Nat. Hazards Earth Syst. Sci.* **2011**, *11*, 2307–2320, doi:10.5194/nhess-11-2307-2011.
29. Sodemann, H.; Schwierz, C.; Wernli, H. Interannual variability of Greenland winter precipitation sources: Lagrangian moisture diagnostic and North Atlantic Oscillation influence. *J. Geophys. Res.* **2008**, *113*, D03107, doi:10.1029/2007JD008503.
30. Lélé, M.I.; Leslie, L.M.; Lam, P.J. Analysis of Low-Level Atmospheric Moisture Transport Associated with the West African Monsoon. *J. Clim.* **2015**, *28*, 4414–4430, doi:10.1175/jcli-d-14-00746.1.



© 2016 by the authors; licensee MDPI, Basel, Switzerland. This article is an open access article distributed under the terms and conditions of the Creative Commons by Attribution (CC-BY) license (<http://creativecommons.org/licenses/by/4.0/>).